



OPEN

Comparative analysis and evaluation of wild and cultivated *Radix Fici Simplicissimae* using an UHPLC-Q-Orbitrap mass spectrometry-based metabolomics approach

Kai-Xin Guo¹, Yan-Fang Li¹, Hui Tang¹, Hao-Yang Wei¹, Wei Zeng¹, Xiao-Cui Yang², Yan Luo¹✉ & Xue-Hong Ke^{1,3}✉

Radix Fici Simplicissimae (RFS) is widely studied, and is in demand for its value in medicines and food products, with increased scientific focus on its cultivation and breeding. We used ultra-high-performance liquid chromatography quadrupole-orbitrap mass spectrometry-based metabolomics to elucidate the similarities and differences in phytochemical compositions of wild *Radix Fici Simplicissimae* (WRFS) and cultivated *Radix Fici Simplicissimae* (CRFS). Untargeted metabolomic analysis was performed with multivariate statistical analysis and heat maps to identify the differences. Eighty one compounds were identified from WRFS and CRFS samples. Principal component analysis and orthogonal partial least squares discrimination analysis indicated that mass spectrometry could effectively distinguish WRFS from CRFS. Among these, 17 potential biomarkers with high metabolic contents could distinguish between the two varieties, including seven phenylpropanoids, three flavonoids, one flavonol, one alkaloid, one glycoside, and four organic acids. Notably, psoralen, apigenin, and bergapten, essential metabolites that play a substantial pharmacological role in RFS, are upregulated in WRFS. WRFS and CRFS are rich in phytochemicals and are similar in terms of the compounds they contain. These findings highlight the effects of different growth environments and drug varieties on secondary metabolite compositions and provide support for targeted breeding for improved CRFS varieties.

Keywords Discrimination, Metabolomics, Wild *Radix Fici Simplicissimae*, Cultivated *Radix Fici Simplicissimae*, UPLC-Q-Orbitrap HRMS

Radix Fici Simplicissimae (RFS), the dry root of *Ficus hirta* Vahl., often called Guangdong ginseng or Wuzhaolong, is a widely distributed mulberry plant, occurring in Guangdong, Fujian, and Guangxi, in China^{1,2}. RFS is a common medicine used by minority nationalities in the Lingnan region, especially the Yao and Zhuang nationalities³. It was first recorded in the Natural Preparation of Raw Herbs, and its application has beneficial impacts on the spleen and lungs, qi and dampness, muscles, and collateral circulation. Some applications of RFS include spleen deficiency and edema, insufficient food and abdominal distension, limb fatigue and weakness, lung deficiency and phlegm asthma, belching, night sweats, rheumatism and pain, postpartum non-lactation, and bruising⁴⁻⁶.

¹Guangzhou University of Chinese Medicine, Guangzhou 510405, China. ²Qingyuan Traditional Chinese Medicine Hospital, Qingyuan 511500, China. ³Experimental Center, The First Hospital Affiliated to Guangzhou University of Chinese Medicine, Guangzhou University of Chinese Medicine, Jichang Road No. 16, Guangzhou 510405, China. ✉email: 409182103@qq.com; kexuehong@126.com

RFS was included in the 1977 edition of the Chinese Pharmacopoeia, and is a primary medicinal material used in Gongyanping tablets in the Chinese Pharmacopoeia⁷. It is also included in the Quality Standard of Yao Medicinal Materials in the Guangxi Zhuang Autonomous Region (Volume I) (2013 edition)⁸. Recently, with increasing attention being paid by the state to develop minority medicines, Wild *Radix Fici Simplicissimae* (WRFS) has been widely studied and frequently applied as a genuine Yao medicine. The value of RFS in medicine and food products is also increasingly researched and medically applied. RFS resources are primarily wild, but intensive land use and mining have reduced the wild RFS resources despite high market demand, while RFS cultivation has increased⁹. Cai et al.¹⁰ and Huang et al.¹¹ assessed psoralen content as the quality standard of RFS and found great differences in the quality of RFS produced in different regions of Guangdong Province. However, research is lacking on WRFS and Cultivated *Radix Fici Simplicissimae* (CRFS) using technologies such as mass spectrometry combined with chemical pattern recognition, limiting standard development of RFS formulations.

Among several primary metabolomics research technologies, nuclear magnetic resonance (NMR) and chromatography coupled with tandem mass spectrometry (MS) are the most used. MS is used to identify metabolites using rapid, sensitive, and selective qualitative and quantitative methods, and combined with effective sample pretreatment and chromatographic separation, has high sensitivity and specificity. Liquid chromatography–mass spectrometry (LC–MS) uses high-throughput MS screening technology combined with metabolite identification, elucidates relevant biomarkers, and effectively analyzes the product components. Metabolomics combined with stoichiometry is used to monitor changes in the chemical components of traditional Chinese medicines from different sources^{12,13}, growth sites¹⁴, and processing methods^{15,16}, and for quality control (QC) of traditional Chinese medicines^{17–19}.

In the early stage, we established the RFS fingerprint and the detection method of main components by HPLC²⁰. In the present study, we used ultra-high-performance liquid chromatography quadrupole-orbitrap mass spectrometry-based metabolomics to elucidate the similarities and differences in phytochemical compositions of WRFS and CRFS. We aimed to analyze the effects of different growth environments and drug varieties on secondary metabolites and provide insights for targeted breeding of improved CRFS varieties.

Materials and methods

Plant materials

Qingyuan City is in the mountainous area of northern Guangdong Province and is a central residential area of the Yao nationality in China. In this study, 29 batches of RFS were harvested. Seventeen batches of WRFS samples were collected from Qingyuan City (Guangdong Province, China), and twelve CRFS samples were collected from hospitals and pharmacies (Table 1). Professor Yuan Xiaohong of Guangdong Provincial Hospital of Traditional Chinese Medicine identified all the medicinal materials. Among them, WRFS were provided by Qingyuan Traditional Chinese Medicine Hospital in May 2022, and CRFS were provided by Guangzhou First Affiliated Hospital of Traditional Chinese Medicine in June 2022. All samples were collected with the approvals from the respective authorities. The phenotypes of RFS are shown in Fig. 1.

Ethics statement

Collection of *Radix Fici Simplicissimae* in this research material conforms to and complies with the IUCN Policy Statement on Research Involving Species at Risk of Extinction and the Convention on the Trade in Endangered Species of Wild Fauna and Flora. In addition, according to the List of National Key Protected Wild Plants issued by the State Forestry and Grassland Bureau of China, *Radix Fici Simplicissimae*, the experimental material of this study, is not a national key protected wild plant nor an endangered plant species.

Sample preparation and extraction

The samples were ground and sieved (Chinese National Standard Sieve No. 3, R40/3 series) to obtain a homogeneous powder. Then, 0.1 g dried samples were added to a 5 mL volumetric flask, and 5 mL of 50% methanol was added. The mixture was left standing for 60 min and extracted using ultrasound (350 W, 35 kHz) (SK3300LH Ultrasonic Cleaner (Shanghai Kedao Ultrasonic Instrument Co., Ltd.)) for 60 min at 37 °C. Methanol (50%) was added to compensate for the loss in weight. The mixture was centrifuged (13,000 rpm; Thermo Legend Micro17R Centrifuge) for 10 min to obtain a clear solution. Additionally, a reference solution of psoralen and apigenin was prepared using the same method.

To ensure the suitability and stability consistency of MS analysis, a QC sample was prepared by pooling the same volume (10 µL) from every sample. In the entire worklist, one QC sample was inserted into every five test and analysis samples, and six QC injections were given to monitor the repeatability of the analysis. A volume of 3 µL was injected for each sample and QC. Metabolite extraction and detection repeatability were determined by overlapping the total ion flow diagram of MS detection and analysis of different QC samples.

UPLC-Q-Orbitrap HRMS analysis

Liquid chromatography

Ultra-high-performance liquid chromatography quadrupole-orbitrap mass spectrometry (UPLC-Q-Orbitrap HRMS) analysis was performed on a Thermo QExactive mass spectrometer (Thermo Fisher Scientific, Waltham, MA, USA) equipped with a UPLC system through an electrospray ionization (ESI) interface. Samples were separated on a Thermo Hypersil Gold VANQUISH C18 (2.1 × 100 mm, 3 µm). The mobile phases were eluent A (0.1% formic acid in water, v/v) and eluent B (acetonitrile, v/v). The elution conditions applied were: 0–5 min, 5% B; 5–12 min, 25–80% B; 12–18 min, 80–99% B; 18–20 min, 99–5% B. The flow rate was 0.2 mL/min and sample injection volume was 3 µL. The column was maintained at 40 °C. Mass spectrometric grade formic acid,

Species	Sample no.	Source	Collection time or batch number
WRFS	1	Lianshan County, Qingyuan City, Guangdong Province, China	October 2020
WRFS	2	Lianshan County, Qingyuan City, Guangdong Province, China	October 2020
WRFS	3	Lianshan County, Qingyuan City, Guangdong Province, China	October 2020
WRFS	4	Yingde County, Qingyuan City, Guangdong Province, China	October 2020
WRFS	5	Yingde County, Qingyuan City, Guangdong Province, China	October 2020
WRFS	6	Yingde County, Qingyuan City, Guangdong Province, China	October 2020
WRFS	7	Yingde County, Qingyuan City, Guangdong Province, China	December 2020
WRFS	8	Yingde County, Qingyuan City, Guangdong Province, China	December 2020
WRFS	9	Yingde County, Qingyuan City, Guangdong Province, China	December 2020
WRFS	10	Liannan County, Qingyuan City, Guangdong Province, China	January 2020
WRFS	11	Liannan County, Qingyuan City, Guangdong Province, China	January 2020
WRFS	12	Liannan County, Qingyuan City, Guangdong Province, China	April 2020
WRFS	13	Qingcheng County, Qingyuan City, Guangdong Province, China	April 2020
WRFS	14	Qingcheng County, Qingyuan City, Guangdong Province, China	May 2020
WRFS	15	Qingcheng County, Qingyuan City, Guangdong Province, China	May 2020
WRFS	16	Qingcheng County, Qingyuan City, Guangdong Province, China	December 2020
WRFS	17	Qingcheng County, Qingyuan City, Guangdong Province, China	December 2020
CRFS	18	Heyuan Jinyuan Green Life Co., Ltd. Jinlusheng Traditional Chinese Medicine Factory	220,101
CRFS	19	Guangdong Tiancheng Traditional Chinese Medicine Slices Co., Ltd	210,801
CRFS	20	Zhongshan Xianyitang Traditional Chinese Medicine Slices Co., Ltd	2,107,137
CRFS	21	Zhongshan Xianyitang Traditional Chinese Medicine Slices Co., Ltd	2,109,087
CRFS	22	Zhongshan Xianyitang Traditional Chinese Medicine Slices Co., Ltd	2,202,045
CRFS	23	Zhongshan Xianyitang Traditional Chinese Medicine Slices Co., Ltd	2,202,044
CRFS	24	Zhongshan Xianyitang Traditional Chinese Medicine Slices Co., Ltd	2,108,186
CRFS	25	Zhongshan Xianyitang Traditional Chinese Medicine Slices Co., Ltd	2,107,049
CRFS	26	Zhongshan Xianyitang Traditional Chinese Medicine Slices Co., Ltd	2,111,011
CRFS	27	Zhongshan Xianyitang Traditional Chinese Medicine Slices Co., Ltd	2,109,084
CRFS	28	Traditional Chinese Medicine Slice Factory of Guangdong Pharmaceutical Company	W2422311
CRFS	29	Traditional Chinese Medicine Slice Factory of Guangdong Pharmaceutical Company	W2422312

Table 1. WRFS and CRFS samples from Guangdong province, China. WRFS, Wild Radix Fici Simplicissimae; CRFS, Cultivated Radix Fici Simplicissimae.

chromatographic grade methanol, and acetonitrile were purchased from Merck, Germany; ultrapure water and all other reagents were of analytical grade.

Mass spectrometry

The positive mode conditions were as follows: capillary voltage, 4.00 kV; carrier gas, nitrogen; sheath gas pressure, 3.5 MPa; auxiliary gas pressure, 1.0 MPa; capillary temperature: 320 °C; auxiliary gas heating temperature: 320 °C; primary resolution: 70,000. The negative mode conditions were identical to the positive mode conditions except for the capillary voltage (3.00 kV). The full scan mode was used, and positive and negative ions were detected simultaneously. The scanning range of the positive and negative ion spectra recorded by MS was 80–1200 m/z.

Data analysis

Chemical component identification

For data collection, the samples were detected simultaneously in the first and second scanning modes under positive and negative ions, respectively, using UPLC-Q-Orbitrap HRMS (Thermo Fisher Scientific), and a total ion flow diagram was plotted. According to the pyrolysis spectrum detected in the electrostatic field orbital well analyzer, the accurate relative molecular weight, retention time, and multistage fragment ion information of the compound were obtained using a Compound Discoverer 3.2. The parameters were as follows: for 2D peak detection, 200 was set as the minimum peak area; for 3D peak detection, the peak intensities of low and high energy were set as > 1000 and > 200 counts, respectively; mass error in the range of ± 5 ppm was set for identified compounds; retention time in the range of ± 0.1 min was allowed to match the reference substance²¹. The predicted fragments generated from the structures were matched and identified against the mzCloud database and ChemSpider. Supporting information was obtained from relevant literature in databases such as PubMed.

Multivariate statistical analysis

The differences between WRFS and CRFS were explored using a metabolomics workflow. Multivariate statistical analysis was performed using SIMCA-P 14.0, and unsupervised principal component analysis (PCA) was used to obtain an initial understanding of the relationships between the data matrices. First, PCA was used to show



Figure 1. Phenotype of RFS : CRFS (wild *Radix Fici Simplicissima*) (A,C) and WRFS (cultivated *Radix Fici Simplicissima*) (B,D).

pattern recognition and maximum variation to obtain an overview and classification. Second, the metabolite differences between different varieties of RFS and culture methods were detected using orthogonal projections to latent structures discriminant analysis (OPLS-DA) monitoring. OPLS-DA in ESI⁺ and ESI⁻ modes was performed to obtain the maximum separation between the CRFS and WRFS groups and to explore the potential biochemical markers contributing to the differences. S-plots were created to visualize the OPLS-DA predictive component loading to facilitate model interpretation. The corresponding variable importance for projection (VIP) was calculated in the OPLS-DA model, and VIP values were used to screen the different components. Metabolites with a VIP value of > 1 and a *p*-value of < 0.05 were considered potential markers. A heatmap was generated from these biochemical markers to visualize the variations in differential metabolites in the different groups, and metabolites with significant statistical differences among the classes were used to generate a heatmap in MetaboAnalyst4.0 (www.metaboanalyst.ca)²². We annotated the obtained differential metabolites using the Kyoto Encyclopedia of Genes and Genomes (KEGG) database and identified the corresponding pathways.

Results and discussion

Stability of the UPLC–MS/MS system

QC samples were used to evaluate the stability of the UPLC–MS/MS system. The curve overlaps between the metabolite detection and total ion current were high. The relative standard deviations (RSD) of the areas of all peaks were calculated, and the screening rates of the characteristic RSD < 30% in the positive and negative modes were 98.54% and 98.33%, respectively. These results suggest a high stability of the UPLC–MS/MS system throughout the experiment.

Identity assignment and compound confirmation

Differential analysis in chemical composition between CRFS and WRFS

The chemical profiles of WRFS and CRFS were analyzed using UPLC-Q-Orbitrap HRMS. A total of eighty one compounds were identified or tentatively characterized in ESI⁺ and ESI⁻ modes from WRFS and CRFS. Representative base peak intensity (BPI) chromatograms of the WRFS and CRFS are shown in Fig. 2.

The similarity between the two BPI chromatograms was relatively high. Using Compound Discoverer 3.2 (Table 2), eighty one compounds were characterized from CRFS and WRFS, which were equivalent to [M + H]⁺ and [M - H]⁻ ions and were unambiguously or tentatively identified through a match with accurate molecular weights within a mass accuracy of < 5 ppm. Both types of RFS extracts were rich in compounds with various structural patterns, including flavonoids, coumarins, alkaloids, glycosides, organic acids, and organic acid esters. In addition, the ion chromatograms and mass spectra of psoralen and apigenin standards were compared, as shown in Fig. 3; the secondary fragment peaks were consistent with those of the corresponding compounds in Table 2, indicating the accuracy of compound identification by CD 3.2 software.

PCA is an important method for the dimensionality reduction of data and an unsupervised multivariate statistical pattern recognition method, and may be used to highlight specific samples from all data. The PCA score plots of WRFS and CRFS showed substantial aggregation separation (Fig. 4A,B). To evaluate the differences in RFS between different cultivation methods and to understand the variables responsible for sample separation, we determined the importance of the variables in the OPLS-DA scoring charts, S-charts, permutation tests, and projection values. OPLS-DA differs from PCA because it is a supervised discriminant analysis method with superior classification and prediction capabilities. OPLS-DA uses partial least squares regression to establish a relationship model between metabolite expression and sample categories to predict the sample categories. Therefore, the OPLS-DA method was used to determine the differences between WRFS and CRFS components. The WRFS samples were separated from CRFS samples in the OPLS-DA score plot (Fig. 4C,D), suggesting differences in biochemistry between WRFS and CRFS.

The data processed by Compound Discoverer 3.2 was imported into SIMCA-P 14.0 software, and unsupervised PCA was used to evaluate the classification trend and differences between groups. The R²X of the model in positive and negative ion mode was greater than 0.4 (0.492 and 0.522, respectively), indicating that the model was stable and reliable. Two hundred rounds of random permutations were performed to verify the established

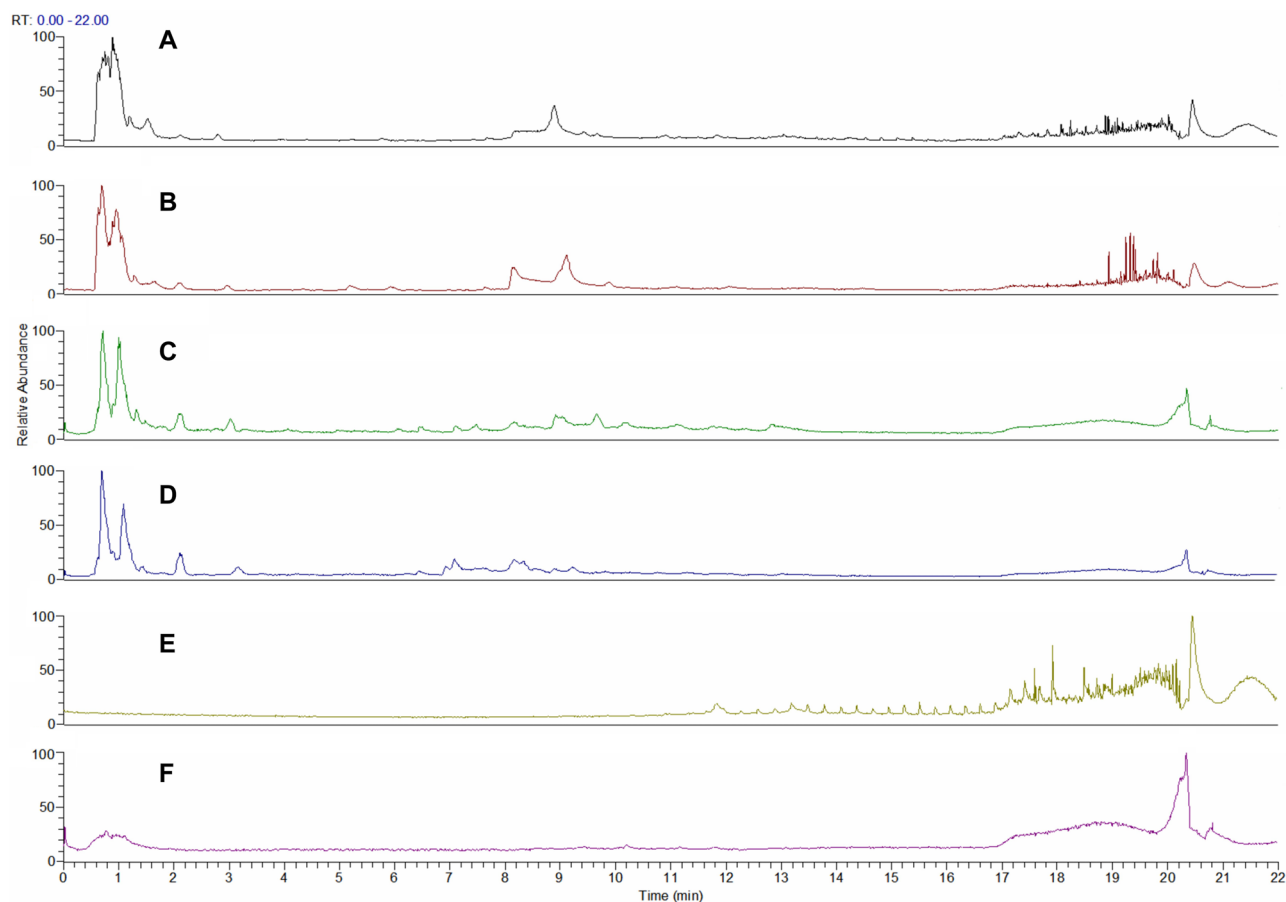


Figure 2. Base peak intensity (BPI) chromatograms of WRFS and CRFS in ESI⁺ and ESI⁻ modes: (A) WRFS in ESI⁺ mode; (B) CRFS in ESI⁺ mode; (C) WRFS in ESI⁻ mode; (D) CRFS in ESI⁻ mode; (E) Blank control in ESI⁺ mode (50% methanol solution); (F) Blank control in ESI⁻ mode (50% methanol solution).

No	RT (min)	Tentative identification of compound	Formula	Observed neutral mass (Da)	Observed m/z	Error (ppm)	Adducts	Main fragments via MS/MS
1	0.616	D-(+)-Proline	C ₅ H ₉ NO ₂	115.06313	116.07060	-1.74	+H	116.07036; 70.06546
2	0.707	Cytosine	C ₄ H ₅ N ₃ O	111.04325	112.05054	-0.11	+H	112.05058
3	0.725	Betaine	C ₅ H ₁₁ NO ₂	117.0789	118.08626	-0.68	+H	118.08641
4	0.729	Trigonelline	C ₇ H ₇ NO ₂	137.04732	138.05495	-2.64	+H	138.05447
5	0.934	DL-Carnitine	C ₇ H ₁₅ NO ₃	161.10478	162.11247	-2.55	+H	162.11206; 103.03913
6	0.994	Guanine	C ₅ H ₅ N ₅ O	151.04907	152.05669	-2.26	+H	152.05637
7	1.039	Nicotinic acid	C ₆ H ₅ NO ₂	123.03186	124.03930	-1.33	+H	124.03917
8	1.21	Hordeanine	C ₁₀ H ₁₅ NO	165.11495	166.12264	-2.48	+H	166.12209; 121.06458
9	1.495	5-Hydroxymethyl-2-furaldehyde	C ₆ H ₆ O ₃	126.03152	127.03897	-1.34	+H	127.03873; 109.02834; 81.03376
10	1.506	L-Isoleucine	C ₆ H ₁₃ NO ₂	131.09436	132.10191	-2.04	+H	132.10146; 86.09663
11	1.676	2-(3-methoxyphenyl)acetamide	C ₉ H ₁₁ NO ₂	165.07861	166.08626	-2.26	+H	166.12196; 121.06451
12	2.092	L-Phenylalanine	C ₉ H ₁₁ NO ₂	165.07859	166.08626	-2.33	+H	166.08554; 120.08066
13	2.218	Pyrogallol	C ₆ H ₆ O ₃	126.03149	127.03897	-1.6	+H	127.03868; 109.02834; 81.03374
14	4.124	(1r,3R,4 s,5S)-4-[[[(2E)-3-(3,4-dihydroxyphenyl)prop-2-enoyl]oxy]-1,3,5-trihydroxycyclohexane-1-carboxylic acid	C ₁₆ H ₁₈ O ₉	354.09409	355.10236	-2.8	+H	355.10049; 163.03877
15	4.71	Scopoletin	C ₁₀ H ₈ O ₄	192.04188	193.04954	-1.99	+H	193.04912; 178.02559
16	4.926	7-Hydroxycoumarin	C ₉ H ₆ O ₃	162.03126	163.03897	-2.67	+H	163.03860; 119.02550
17	5.225	Vitexin	C ₂₁ H ₂₀ O ₁₀	432.1045	433.11292	-2.66	+H	433.11154; 313.06964; 283.05920
18	5.331	Orientin	C ₂₁ H ₂₀ O ₁₁	448.09911	449.10784	-3.23	+H	449.10388; 329.06363; 299.05377
19	5.591	Vanillin	C ₈ H ₈ O ₃	152.04697	153.05462	-2.43	+H	153.05408; 125.05941; 111.04398; 93.03362
20	5.953	1,5-Anhydro-1-[5,7-dihydroxy-3-(4-hydroxyphenyl)-4-oxo-4H-chromen-8-yl]hexitol	C ₂₁ H ₂₀ O ₁₀	432.10426	433.11292	-3.21	+H	433.10980; 313.06921; 283.05884; 337.06882
21	7.673	7,8-Dihydroxy-4-methyl coumarin	C ₁₀ H ₈ O ₄	192.04184	193.04954	-2.19	+H	193.04921; 175.03865
22	7.871	Luteolin	C ₁₅ H ₁₀ O ₆	286.0469	287.05501	-2.92	+H	287.05423
23	7.942	(2S)-2-(2-hydroxypropan-2-yl)-2H,3H,7H-furo[3,2-g]chromen-7-one	C ₁₄ H ₁₄ O ₄	246.08845	247.09649	-3.07	+H	247.09590; 229.08540; 175.03862
24	8.049	Eriodictyol	C ₁₅ H ₁₂ O ₆	288.06238	289.07066	-3.5	+H	289.06949; 163.03838; 153.01772
25	8.101	Naringenin	C ₁₅ H ₁₂ O ₅	272.06761	273.07575	-3.16	+H	273.07535; 153.01807; 147.04388
26	8.289	Psoralen	C ₁₁ H ₆ O ₃	186.03114	187.03897	-2.98	+H	187.03816; 143.04860; 131.04869
27	8.418	Apigenin	C ₁₅ H ₁₀ O ₅	270.05202	271.06010	-2.96	+H	271.05933
28	8.559	Apocynin	C ₉ H ₁₀ O ₃	166.06277	167.07027	-1.32	+H	167.06989
29	8.98	Diosmetin	C ₁₆ H ₁₂ O ₆	300.06233	301.07066	-3.52	+H	301.06989; 286.04636
30	9.716	Bergapten	C ₁₂ H ₈ O ₄	216.04168	217.04954	-2.69	+H	217.04901; 202.02550
31	10.198	Chrysin	C ₁₅ H ₁₀ O ₄	254.05736	255.06519	-2.16	+H	255.06454
32	10.201	Trioxsalen	C ₁₄ H ₁₂ O ₃	228.0781	229.08592	-2.41	+H	229.08533
33	11.24	Benzophenone	C ₁₃ H ₁₀ O	182.0727	183.08044	-2.57	+H	183.07977; 105.03344
34	11.884	Psoralidin	C ₂₀ H ₁₆ O ₅	336.0985	337.10705	-3.79	+H	337.10547
35	12.321	3,5-di-tert-Butyl-4-hydroxybenzaldehyde	C ₁₅ H ₂₂ O ₂	234.16121	235.16926	-3.27	+H	235.16846; 179.10611
36	12.338	5-hydroxy-2-(4-hydroxyphenyl)-8,8-dimethyl-4H,8H-pyrano[3,2-g]chromen-4-one	C ₂₀ H ₁₆ O ₅	336.09858	337.10705	-3.56	+H	337.10587; 283.05927
37	12.529	Cryptotanshinone	C ₁₉ H ₂₀ O ₃	296.14038	297.14852	-2.92	+H	297.14764; 251.14246
38	0.675	D-(-)-Mannitol	C ₆ H ₁₄ O ₆	182.07827	181.07176	-4.21	-H	181.07089; 101.02327; 89.02323; 71.01263
39	0.785	Gluconic acid	C ₆ H ₁₂ O ₇	196.05783	195.05103	-2.42	-H	195.05052; 129.01845; 75.00767
40	0.803	D-(-)-Quinic acid	C ₇ H ₁₂ O ₆	192.06259	191.05611	-4.16	-H	191.05530; 85.02831
41	0.846	D-Glucose 6-phosphate	C ₆ H ₁₃ O ₉ P	260.02925	259.02244	-1.8	-H	259.02206; 96.96844; 78.95784

Continued

No	RT (min)	Tentative identification of compound	Formula	Observed neutral mass (Da)	Observed m/z	Error (ppm)	Adducts	Main fragments via MS/MS
42	1.078	α,α -Trehalose	C ₁₂ H ₂₂ O ₁₁	342.11581	341.10894	-1.16	-H	341.10867; 179.05527; 119.03397; 113.02333; 101.02331; 89.02327; 71.01267; 59.01268
43	1.401	Citric acid	C ₆ H ₈ O ₇	192.02631	191.01973	-3.62	-H	191.01921; 111.00783; 87.00772; 85.02847
44	2.082	3-Hydroxy-3-(methoxycarbonyl)pentanedioic acid	C ₇ H ₁₀ O ₇	206.04198	205.03538	-3.25	-H	205.03505; 111.00767; 87.00760
45	2.621	3-[3-(beta-D-Glucopyranosyloxy)-2-hydroxyphenyl]propanoic acid	C ₁₅ H ₂₀ O ₉	344.11042	343.10346	-0.91	-H	343.10345; 181.04984; 163.03908; 137.05981
46	3.307	Quercetin	C ₁₅ H ₁₀ O ₇	302.04235	301.03538	-0.99	-H	301.03494; 151.00244
47	3.64	Caffeic acid	C ₉ H ₈ O ₄	180.04157	179.03498	-3.81	-H	179.03464; 135.04442
48	4.159	Catechin	C ₁₅ H ₁₄ O ₆	290.07881	289.07176	-0.8	-H	289.07126; 245.08139
49	4.25	Chlorogenic acid	C ₁₆ H ₁₈ O ₉	354.09497	353.08781	-0.33	-H	353.08823; 191.05576
50	4.397	2-(Acetylamino)hexanoic acid	C ₈ H ₁₅ NO ₃	173.10442	172.09792	-4.45	-H	172.09688; 130.08630
51	4.601	Fraxetin	C ₁₀ H ₈ O ₅	208.03666	207.0299	-2.49	-H	207.02928; 192.00574
52	4.76	4-Methylumbelliferone	C ₁₀ H ₈ O ₃	176.04658	175.04007	-4.32	-H	175.03926
53	4.783	(1 ξ)-1,5-Anhydro-1-[2-(3,4-dihydroxyphenyl)-5,7-dihydroxy-4-oxo-4H-chromen-8-yl]-D-galactitol	C ₂₁ H ₂₀ O ₁₁	448.10026	447.09329	-0.66	-H	447.09293; 357.06134; 327.05075; 299.05521; 298.04642; 297.04022
54	5.027	(9R,10R)-10-hydroxy-8,8-dimethyl-9-[(2S,3R,4S,5S,6R)-3,4,5-trihydroxy-6-(hydroxymethyl)oxan-2-yl]oxy]-2H,8H,9H,10H-pyrano[2,3-h]chromen-2-one	C ₂₀ H ₂₄ O ₁₀	424.1365	423.12967	-1.06	-H	423.12885; 179.05565; 89.02407; 71.01264; 59.01350
55	5.387	2-(acetylamino)-3-(1H-indol-3-yl)propanoic acid	C ₁₃ H ₁₄ N ₂ O ₃	246.10008	245.09317	-1.48	-H	245.09259; 203.08188; 116.03413; 116.04924; 98.02341; 74.02351; 70.02863; 58.02859
56	5.445	Cnidioside A	C ₁₇ H ₂₀ O ₉	368.11046	367.10346	-0.75	-H	367.10306; 205.04997; 161.05986
57	5.516	3-[4-(beta-D-Glucopyranosyloxy)-6-methoxy-1-benzofuran-5-yl]propanoic acid	C ₁₈ H ₂₂ O ₁₀	398.1212	397.11402	-0.25	-H	397.11465; 235.06100; 191.07083; 176.04729
58	5.521	Suberic acid	C ₈ H ₁₄ O ₄	174.08848	173.08193	-4.21	-H	173.08125; 111.08056
59	6.128	Isovanillic acid	C ₈ H ₈ O ₄	168.04145	167.03498	-4.84	-H	167.03418; 152.01070
60	6.259	2,4,6-Trihydroxy-2-(4-hydroxybenzyl)-1-benzofuran-3(2H)-one	C ₁₅ H ₁₂ O ₆	288.06329	287.05611	-0.36	-H	287.05649; 259.06131; 125.02356
61	6.904	Azelaic acid	C ₉ H ₁₆ O ₄	188.10412	187.09758	-3.92	-H	187.09683; 125.09612
62	7.425	Diplosal acetate	C ₁₆ H ₁₂ O ₆	300.06303	299.05611	-1.19	-H	137.02335
63	7.839	Ferulic acid	C ₁₆ H ₁₀ O ₄	194.05724	193.05063	-3.47	-H	193.04990
64	8.196	Genistein	C ₁₅ H ₁₀ O ₅	270.0527	269.04555	-0.44	-H	269.04538
65	8.546	Corchorifatty acid F	C ₁₈ H ₃₂ O ₅	328.22484	327.2177	-0.42	-H	327.21732
66	9.094	Dodecanedioic acid	C ₁₂ H ₂₂ O ₄	230.15147	229.14453	-1.46	-H	229.14404; 230.414699; 211.13297
67	9.233	Mycophenolic acid	C ₁₇ H ₂₀ O ₆	320.1259	319.11871	-0.28	-H	319.11868; 191.03410
68	9.318	Hispidulin	C ₁₆ H ₁₂ O ₆	300.06313	299.05611	-0.87	-H	299.05582; 284.03232
69	9.792	(15Z)-9,12,13-Trihydroxy-15-octadecenoic acid	C ₁₈ H ₃₄ O ₅	330.24045	329.23335	-0.52	-H	329.23294; 171.10173
70	10.085	Taurochenodeoxycholic acid	C ₂₆ H ₄₅ NO ₆ S	499.29649	498.28948	-0.54	-H	498.28958
71	10.247	Monobutyl phthalate	C ₁₂ H ₁₄ O ₄	222.08874	221.08193	-2.12	-H	221.08136; 177.09140; 149.09613; 134.03627; 121.02839; 71.04902; 69.03339
72	10.749	Chrysin	C ₁₅ H ₁₀ O ₄	254.05765	253.05063	-1	-H	253.05031
73	11.286	Asiatic acid	C ₃₀ H ₄₈ O ₅	488.34964	487.3429	-1.09	-H	487.34369
74	12.666	N-(3-Chloro-4-morpholinophenyl)-6-oxo-1,4,5,6-tetrahydro-3-pyridazinocarboxamide	C ₁₅ H ₁₇ ClN ₄ O ₃	336.09964	335.09164	2.15	-H	335.09204
75	12.871	16-Hydroxyhexadecanoic acid	C ₁₆ H ₃₂ O ₃	272.23496	271.22787	-0.7	-H	271.22763
76	13.021	Oleic acid alkyne	C ₁₈ H ₃₀ O ₂	278.22431	277.2173	-0.99	-H	277.21695

Continued

No	RT (min)	Tentative identification of compound	Formula	Observed neutral mass (Da)	Observed m/z	Error (ppm)	Adducts	Main fragments via MS/MS
77	13.05	Dodecyl sulfate	C ₁₂ H ₂₆ O ₄ S	266.15496	265.1479	-0.84	-H	265.14767; 96.95897
78	13.303	(R)-3-Hydroxy myristic acid	C ₁₄ H ₂₈ O ₃	244.20354	243.19657	-1.26	-H	243.19693; 59.01270
79	14.709	Ursolic acid	C ₃₀ H ₄₈ O ₃	456.35989	455.35307	-0.99	-H	455.35260
80	15.503	Myristyl sulfate	C ₁₄ H ₃₀ O ₄ S	294.18635	293.1792	-0.43	-H	293.17935; 96.95897
81	15.738	Linoleic acid	C ₁₈ H ₃₂ O ₂	280.2402	279.23295	-0.13	-H	279.23276

Table 2. UPLC-Q-Orbitrap HRMS-based determination of chemical composition of CRFS and WRFS cultivated in different ways.

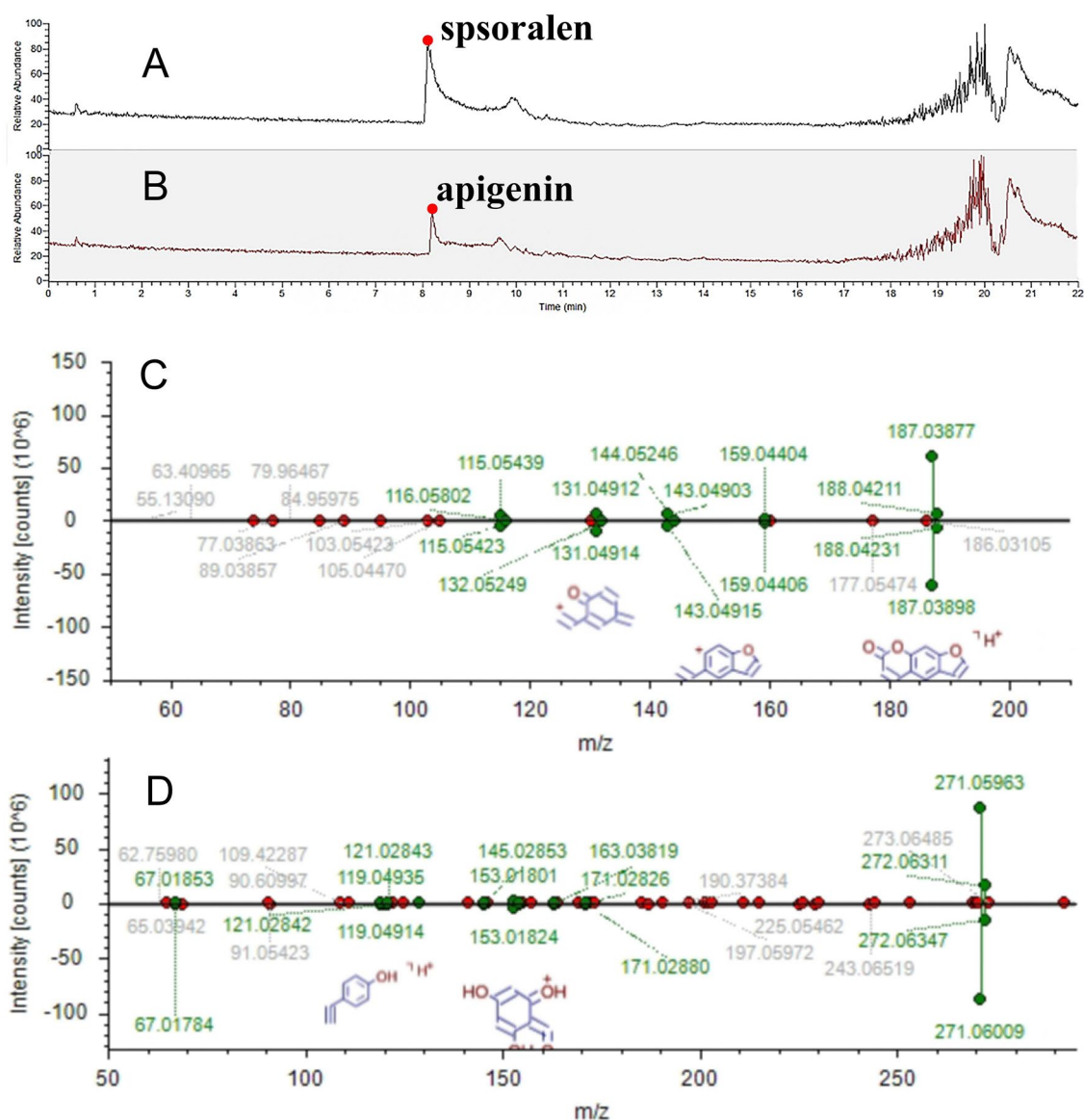


Figure 3. Ion chromatogram of sporsalen in ESI⁺ mode (A); Ion chromatogram of apigenin in ESI⁺ mode (B); Mass spectra of psoralen (C) and apigenin (D).

OPLS-DA model, indicating that the model was reliable (ESI⁺: R²X = 0.359, R²Y = 0.975 and Q² = 0.926; ESI⁻: R²X = 0.333, R²Y = 0.945 and Q² = 0.892, respectively) (Fig. 4E,F). Variables with VIP values of > 1 and *p* < 0.05 in the nonparametric test were considered potential biochemical markers between WRFS and CRFS. (Fig. 4G,H).

A heatmap was generated based on these markers to evaluate them systematically and intuitively (Fig. 5), and to show the strength of potential chemical markers between two samples. The close relationship of 17 potential markers is illustrated by combining the identification results as mentioned above. The samples were divided into two categories, WRFS and CRFS, and the results were consistent with those of the PCA. The 17 potential

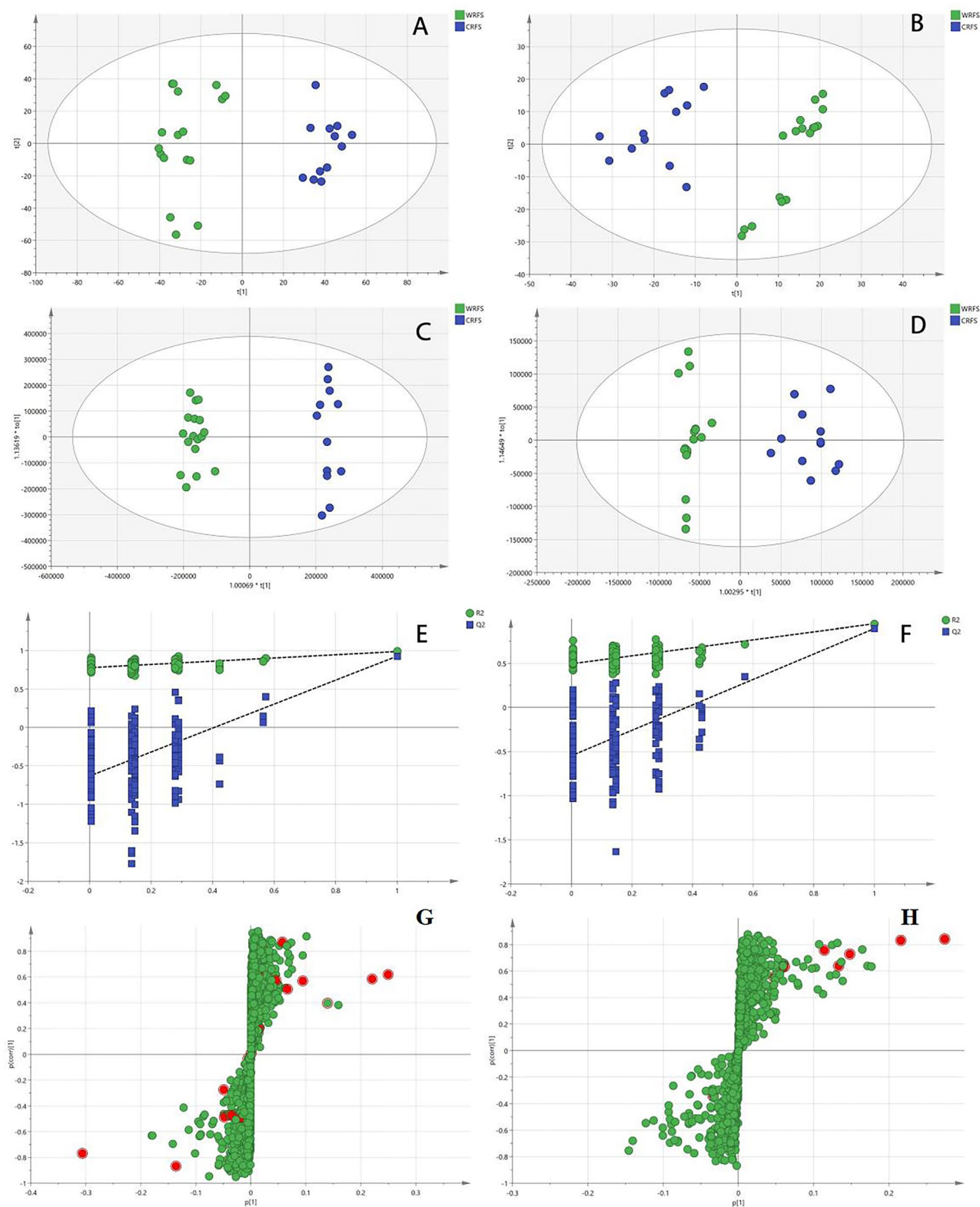


Figure 4. Principal component analysis (PCA) of WRFS and CRFS in ESI⁺ (A) and ESI⁻ (B) mode. OPLS-DA score plot with multivariate statistical analysis WRFS and CRFS in ESI⁺ (C) and ESI⁻ (D) mode. Cross-validation plot of OPLS-DA model with 200 permutation tests in ESI⁺ (E) and ESI⁻ (F) mode. OPLS-DA S-plot in ESI⁺ (G) and ESI⁻ (H) mode. (The red marked points in red of the S-plot graph G and H are potential chemical markers).

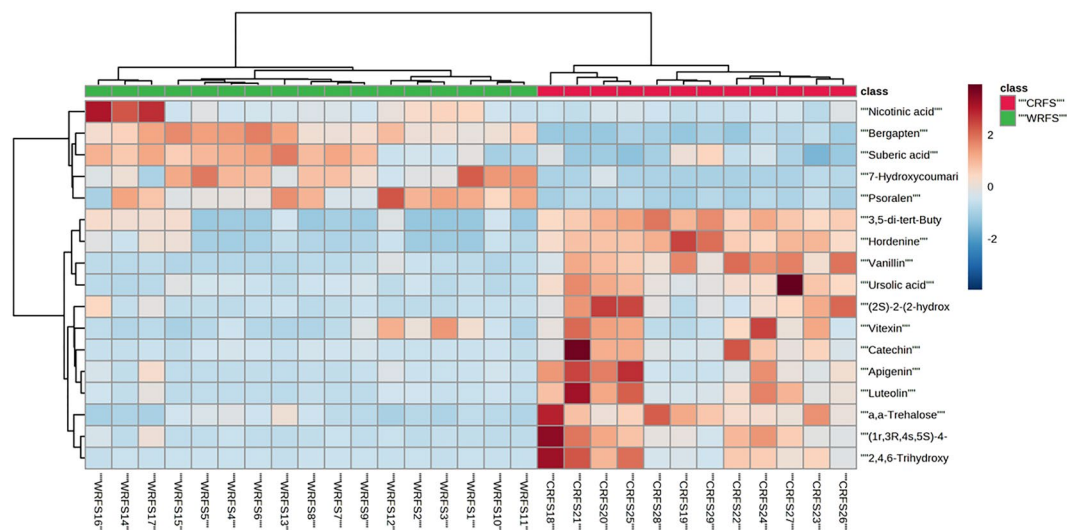


Figure 5. Heatmap of WRFS and CRFS metabolite content.

differential metabolites that could be considered as potential chemical markers for WRFS and CRFS were compounds 7, 8, 14, 16, 17, 19, 22, 23, 26, 27, 30, 35, 42, 48, 58, 60, and 79 (Table 3). The color indicates the signal strength of each metabolite; the darker the red, the greater the extent to which the metabolite appears above the average level of the sample, and blue indicates that the metabolite is at a lower level.

Kyoto Encyclopedia of Genes and Genomes analysis of differential metabolites

The KEGG database integrates genome, chemistry, and system function information and is a comprehensive dataset of metabolic pathway information^{23–25}. The metabolic pathways are classified into different modules according to their functions, such as glycolysis, carbohydrate, TCA cycle, nucleoside and amino acid, organic compound and enzyme biodegradation, and other comprehensive metabolic pathways. Among the 17 differential metabolites, 14 were annotated to the KEGG database, 11 of which were annotated 29 times to KEGG pathways (Table 4). After removing duplication, 15 KEGG pathways were identified. Phenylpropanoid biosynthesis in the KEGG pathway is an example (Fig. 6).

No.	Differential metabolite	Formula	VIP	Fold-change	Type	p-Value
7	Nicotinic acid	$C_6H_5NO_2$	1.404	2.507	Up	1.101E-02
8	Hordenine	$C_{10}H_{15}NO$	4.194	0.205	Down	2.708E-07
14	(1 <i>r</i> ,3 <i>R</i> ,4 <i>s</i> ,5 <i>S</i>)-4-[[<i>(2E)</i> -3-(3,4-dihydroxyphenyl)prop-2-enoyl]oxy]-1,3,5-trihydroxycyclohexane-1-carboxylic acid	$C_{16}H_{18}O_9$	1.243	0.109	Down	1.086E-03
16	7-Hydroxycoumarin	$C_9H_6O_3$	1.610	13.176	Up	3.254E-06
17	Vitexin	$C_{21}H_{20}O_{10}$	1.071	0.439	Down	2.384E-02
19	Vanillin	$C_8H_8O_3$	1.383	0.101	Down	1.563E-05
22	Luteolin	$C_{15}H_{10}O_6$	1.595	0.109	Down	1.583E-03
23	(2 <i>S</i>)-2-(2-hydroxypropan-2-yl)-2 <i>H</i> ,3 <i>H</i> ,7 <i>H</i> -furo[3,2- <i>g</i>]chromen-7-one	$C_{14}H_{14}O_4$	1.117	0.177	Down	3.224E-03
26	Psoralen	$C_{11}H_6O_3$	22.854	7.535	Up	1.952E-06
27	Apigenin	$C_{15}H_{10}O_5$	4.019	4.019	Up	6.356E-03
30	Bergapten	$C_{12}H_8O_4$	10.046	8.541	Up	7.922E-10
35	3,5-di-tert-Butyl-4-hydroxybenzaldehyde	$C_{15}H_{22}O_2$	1.034	0.271	Down	7.997E-09
42	α,α -Trehalose	$C_{12}H_{22}O_{11}$	9.809	0.262	Down	8.921E-05
48	Catechin	$C_{15}H_{14}O_6$	2.225	0.128	Down	7.591E-03
58	Suberic acid	$C_8H_{14}O_4$	1.423	2.035	Up	1.594E-04
60	2,4,6-Trihydroxy-2-(4-hydroxybenzyl)-1-benzofuran-3(2 <i>H</i>)-one	$C_{15}H_{12}O_6$	5.414	0.042	Down	2.505E-03
79	Ursolic acid	$C_{30}H_{48}O_3$	1.114	0.260	Down	1.515E-03

Table 3. Seventeen differential metabolites. Up: compared with CRFS, the corresponding metabolite was upregulated in WRFS. Down: compared with CRFS, the corresponding metabolite was downregulated in WRFS.

KEGG pathway	ID annotation	Number	Differential metabolite	Matching IDs
Biosynthesis of phenylpropanoids	map01061	5	Vanillin, apigenin, bergapten;(2S)-2-(2-hydroxypropan-2-yl)-2H,3H,7H-furo[3,2-g]chromen-7-one, psoralen	C00755 C01477 C01557 C09276 C09305
Flavonoid biosynthesis	map00941	3	Apigenin, vitexin, luteolin	C01460 C01477 C01514
Flavone and flavonol biosynthesis	map00944	2	Apigenin, luteolin	C01477 C01514
Biosynthesis of secondary metabolites	map01110	6	Apigenin, bergapten, psoralen, luteolin, nicotinic acid, 7-hydroxycoumarin	C00253 C01477 C01514 C01557 C05851 C09305
Nicotinate and nicotinamide metabolism	map00760	1	Nicotinic acid	C00253
Tropane, piperidine, and pyridine alkaloid biosynthesis	map00960	1	Nicotinic acid	C00253
Biosynthesis of alkaloids derived from ornithine, lysine, and nicotinic acid	map01064	1	Nicotinic acid	C00253
2,4-Dichlorobenzoate degradation	map00623	1	Vanillin	C00755
Starch and sucrose metabolism	map00500	1	α,α -Trehalose	C01083
Phosphotransferase system (PTS)	map02060	1	α,α -Trehalose	C01083
Phenylpropanoid biosynthesis	map00940	1	7-Hydroxycoumarin	C05851
Tyrosine metabolism	map00350	1	Hordenine	C06199
ABC transporters	map02010	1	α,α -Trehalose	C01083
Biosynthesis of alkaloids derived from the shikimate pathway	map01063	1	Vanillin	C00755
Metabolic pathways	map01100	3	Apigenin, luteolin, nicotinic acid	C00253 C01477 C01514

Table 4. Categories of 14 differential metabolite-annotated KEGG pathways. ID Annotation, ID of KEGG pathway; Number, the number of metabolites that can be annotated to the corresponding KEGG pathways; Matching IDs, Number of compounds in the KEGG pathway.

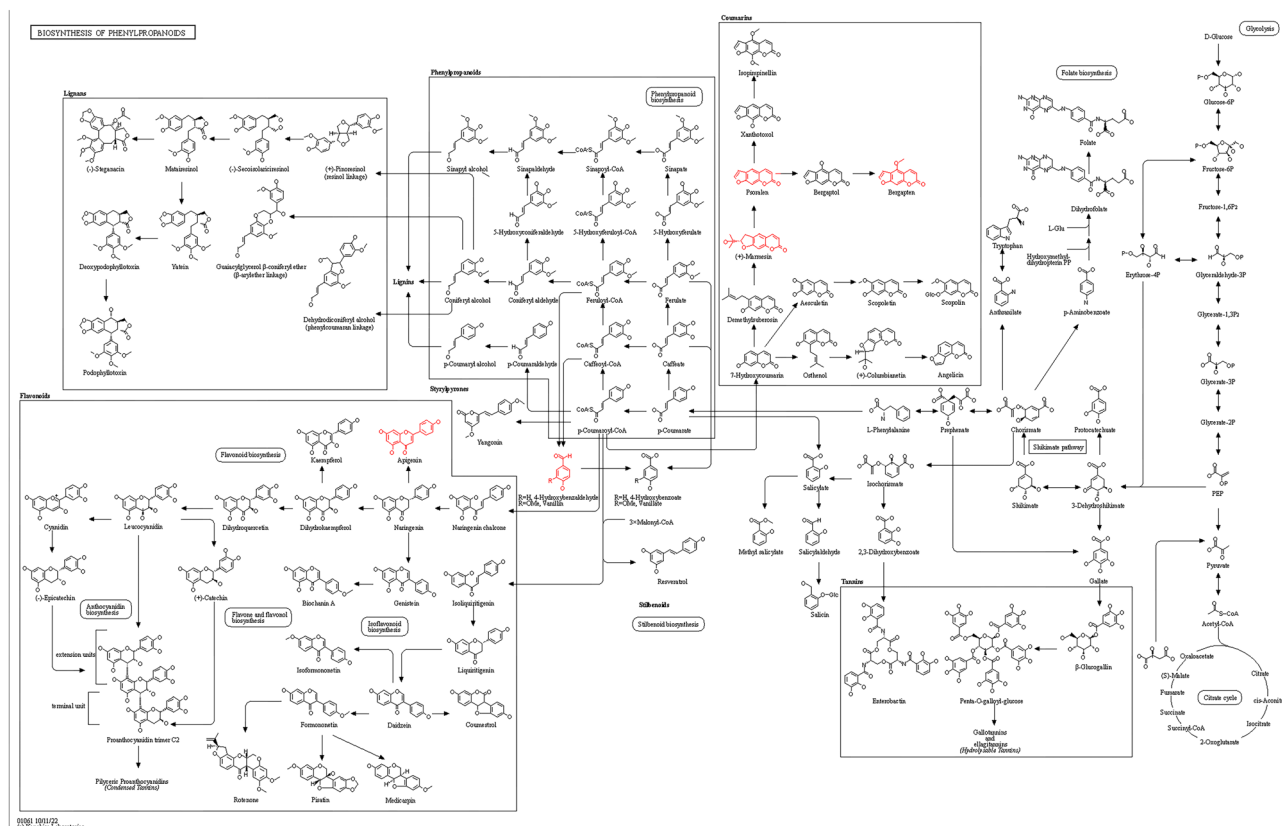


Figure 6. Phenylpropanoid biosynthesis. The compounds marked with red are differential metabolites belonging to phenylpropanes.

Discussion

This study, a metabolomics study based on UPLC-Q-Orbitrap HRMS combined with multivariate statistical analysis revealed substantial differences in the compound compositions of WRFS and CRFS. The results of the identification and analysis of eighty one compounds showed distinct chemical profiles between WRFS and CRFS samples from different cultivation methods. Moreover, the identification results of these compounds in this study are consistent with those of Cheng Jun et al.^{26,27}, which proves that RFS mainly contains phenylpropanoids, flavonoids, coumarins and other substances. Moreover, the chemical composition identification of RFS by Lao et al.²⁸ and Zhao et al.²⁹ showed that Vitexin, Vanillin, Luteolin, Psoralen, Apigenin, Bergapten, Ursolic acid and so on (17 potential differences between CRFS and WRFS) were consistent with our identification results. Using multivariate statistical analysis and a heatmap, WRFS and CRFS showed remarkable discrimination. Many markers exhibited different expression levels between the two samples. Psoralen, bergapten, and apigenin were upregulated in WRFS, and the content of these three active substances was much higher in WRFS than in CRFS. Many researchers have found that Psoralen, bergapten, and apigenin can be used as a quality marker of RFS, and it is the active ingredient with the highest content^{30,31}.

Radix Fici Simplicissima, one of ten famous medicines in Lingnan region, has been proven to play a role in protecting the liver, relieving inflammation, and having antioxidant and anti-cancer activities³². The ethanol extract of RFS can protect the liver of mice from alcohol-induced liver injury, probably by inducing and regulating downstream antioxidant factors, and also by suppressing the abnormal activation of CYP2E1 protein, reducing oxidative stress, and ultimately reducing the damage to the liver caused by alcohol³³. Zhou Tiannong et al.³⁴ found that compared with the control group, the water extract of RFS can significantly inhibit the increase of abdominal capillary diameter and improve the pain threshold of mice. It can also reduce the levels of alanine aminotransferase (ALT) and aspartate aminotransferase (AST) in mouse serum, which have good anti-inflammatory, analgesic, and liver protective effects. Deep research on the active components of RFS shows that it mainly consists of phenolic acids, terpenoids, flavonoids, coumarins, and phenolic acids^{26,35}. Many scholars^{36–39} believe that the active components with a pharmacological effect that can be used as quality markers are psoralen, biflavonoids, and apigenin. Therefore, it should be studied as the main index. Psoralen, biflavonoids and apigenin have anti-tumor^{40,41}, neuroprotective⁴², anti-inflammatory⁴³, antioxidant and other pharmacological activities, which can be used to treat cancer, insomnia, Alzheimer's disease, rheumatoid arthritis, and aging. Psoralen and biflavonoids can prevent osteoporosis⁴⁴, while apigenin can enhance immunity and prevent hypertension, arteriosclerosis, and cardiovascular and cerebrovascular diseases⁴⁵. Because these different metabolites play an important role in health-related effects, these three components are very important for the quality evaluation of RFS. Our results show that the quality of WRFS is better than that of CRFS.

The main metabolic pathways that differ between WRFS and CRFS include primary and secondary metabolite biosynthesis. Psoralen, apigenin, and biflavonoids are annotated in multiple KEGG pathways related to phenylpropanoid biosynthesis, flavonoid biosynthesis, flavone and flavonol biosynthesis, and so on. Phenylpropanoid biosynthesis is an important metabolic process in humans, mainly involving the metabolism of amino acids such as phenylalanine and tyrosine. The process involves participation of various enzymes in catalyzing reactions to convert phenylalanine into other amino acids such as tyrosine. This biochemical process is crucial for the normal functioning of many physiological functions in the human body⁴⁶. Flavonoids are an important branch of the phenylpropanoid metabolic pathway. The biosynthesis of flavonoids begins with phenylalanine, which is catalyzed by enzymes such as chalcone synthase to produce chalcone. Subsequently, the chalcone isomerizes into flavonoids, which then produces a variety of other flavonoid compounds, such as flavonols, isoflavones, and anthocyanins⁴⁷. In addition, flavonoid and flavonols are two important components of flavonoids. Therefore, the results of this study provide clues for analyzing these metabolites and their metabolic networks in RFS. The variety and quantity of RFS collected in this study are limited, and its limitation should be attributed to the lack of sufficient sample size to support the research results, which can be expanded for further exploration.

This study showed that WRFS was superior to CRFS in quality, and explained the effects of different growth environments and drug varieties on secondary metabolites, and provides insights for further targeted breeding of improved CRFS varieties.

Conclusion

In this study, a UPLC-Q-Orbitrap HRMS method was established and successfully applied to determine the component profiles of various RFS samples grown under different cultivation methods. Using multivariate statistical analysis and heat maps, WRFS and CRFS were shown to have significant differences. Psoralen, bergapten, and apigenin were significantly upregulated in WRFS compared to CRFS. Due to the important roles of these differential metabolites, our results indicate that the quality of WRFS is superior to that of CRFS, and this strategy will benefit the process of quality evaluation of RFS formulations.

Data availability

All data is available within the article or supplementary material.

Received: 11 October 2023; Accepted: 25 March 2024

Published online: 28 March 2024

References

1. Zhang, R. & Du, J. Research progress of five-fingered peach. *Chin. Mod. Chin. Med.* **41**(05), 48–52. <https://doi.org/10.13424/j.cnki.mtcm.2021.05.008> (2021).

2. Teng, L. L., Qin, H. Z., Xiong, Z. C., Wei, X. & Shi, Y. C. Research on cuttings technology of five-fingered peach for medicinal and edible plants. *J. Trop. Agric. Sci.* **42**(02), 23–30 (2022).
3. Ma, J. & Zhang, H. W. *Collection of Lingnan materia medica* 66p (Science Press, Beijing, 2010).
4. He, L. Y. & Chen, Y. Y. Study on high performance liquid chromatography fingerprint of five-finger peach. *Zhongnan Pharm.* **13**(07), 681–684 (2015).
5. Standards for Chinese medicinal materials in Guangdong Province. (ed. Guangdong Food and Drug Administration), 35–36 (Guangzhou, China: Guangdong Science and Technology Press, 2004).
6. Huang, P. W. *et al.* Research progress on chemical composition, pharmacological effects and clinical application of Chinese medicine *P. quinquen.* *J. Liaoning Univ. Trad. Chin. Med.* **22**(12), 93–96. <https://doi.org/10.13194/j.issn.1673-842x> (2020).
7. Chinese pharmacopoeia (ed. Chinese Pharmacopoeia Commission), 1088 (Beijing, China: The Medicine Science and Technology Press of China, 2020).
8. Quality Standard of Yao Medicinal Materials in Guangxi Zhuang Autonomous Region (ed. Guangxi Food and Drug Administration), 46 (Guangxi, China: Guangxi Science and Technology Press, 2014).
9. Oouyang, X. N. *et al.* Research progress of Lingnan real estate medicinal material five-fingered peach. *For. Pract. Technol. Publ.* **02**, 34–38. <https://doi.org/10.13456/j.cnki.lykt.2021.08.20.0005> (2022).
10. Cai, S. X., Luo, J. & Li, C. Y. Determination of psoralen content in medicinal materials of five-finger peach from 15 different origins in Guangdong Province. *Sci. Technol. Inf.* **17**(06), 201–202. <https://doi.org/10.16661/j.cnki.1672-3791.2019.06.201> (2019).
11. Huang, W. H., Song, Y. G., Li, Z. Y., Liu, X. H. & Liu, D. L. Determination and quality evaluation of psoralen and trace elements in medicinal materials of five-finger peach from different origins in Guangdong. *Western Chin. Med.* **26**(04), 14–16 (2013).
12. Lee, E. J. *et al.* Quality assessment of ginseng by ¹H NMR metabolite fingerprinting and profiling analysis. *J. Agric. Food Chem.* **57**(16), 7513–7522. <https://doi.org/10.1021/jf901675y> (2009).
13. Yang, S. O. *et al.* NMR-based metabolic profiling and differentiation of ginseng roots according to cultivation ages. *J. Pharm. Biomed. Anal.* **58**, 19–26. <https://doi.org/10.1016/j.jpba.2011.09.016> (2012).
14. Toh, D. F., New, L. S., Koh, H. L. & Chan, E. C. Ultra-high performance liquid chromatography/time-of-flight mass spectrometry (UHPLC/TOFMS) for time-dependent profiling of raw and steamed *Panax notoginseng*. *J. Pharm. Biomed. Anal.* **52**(1), 43–50. <https://doi.org/10.1016/j.jpba.2009.12.005> (2010).
15. Sun, J. & Chen, P. Differentiation of *Panax quinquefolius* grown in the USA and China using LC/MS-based chromatographic fingerprinting and chemometric approaches. *Anal. Bioanal. Chem.* **399**(5), 1877–1889. <https://doi.org/10.1007/s00216-010-4586-7> (2011).
16. Li, H. Y. *et al.* In vitro study on the characteristics of bergamot lactone in inhibition of nasopharyngeal carcinoma cancer stem cells. *Pharm. Today.* **29**(08), 515–520 (2019).
17. Qiu, S. *et al.* Nontargeted metabolomic analysis and “commercial-homophyletic” comparison-induced biomarkers verification for the systematic chemical differentiation of five different parts of *Panax ginseng*. *J. Chromatogr. A* **1453**, 78–87. <https://doi.org/10.1016/j.chroma.2016.05.051> (2016).
18. Yao, C. *et al.* UHPLC-Q-TOF-MS-based metabolomics approach to compare the saponin compositions of Xueshuantong injection and Xuesaitong injection. *J. Sep. Sci.* **40**(4), 834–841. <https://doi.org/10.1002/jssc.201601122> (2017).
19. Yu, X. A. *et al.* Influence of different processing times on the quality of *Polygoni Multiflora Radix* by metabolomics based on ultra high performance liquid chromatography with quadrupole time-of-flight mass spectrometry. *J. Sep. Sci.* **40**(9), 1928–1941. <https://doi.org/10.1002/jssc.201600913> (2017).
20. Yang, X. Q. *et al.* Evaluation of the quality of cultivated and wild five-fingered peach based on fingerprint combined with chemochrometry. *China Pharm. J.* **32**(19), 63–69 (2023).
21. Lin, H. *et al.* Comparative analysis of chemical constituents of *Moringa oleifera* leaves from China and India by ultra-performance liquid chromatography coupled with quadrupole-time-of-flight mass spectrometry. *Molecules* **24**(5), 942. <https://doi.org/10.3390/molecules24050942> (2019).
22. Luo, Y. *et al.* Discrimination of *Citrus reticulata* Blanco and *Citrus reticulata* “Chachi” as well as the *Citrus reticulata* “Chachi” within different storage years using ultra high performance liquid chromatography quadrupole/time-of-flight mass spectrometry based metabolomics approach. *J. Pharm. Biomed. Anal.* **15**(171), 218–231. <https://doi.org/10.1016/j.jpba.2019.03.056> (2019).
23. Kanehisa, M. & Goto, S. KEGG: Kyoto encyclopedia of genes and genomes. *Nucleic Acids Res.* **28**(1), 27–30. <https://doi.org/10.1093/nar/28.1.27> (2000).
24. Kanehisa, M. Toward understanding the origin and evolution of cellular organisms. *Protein Sci.* **28**(11), 1947–1951. <https://doi.org/10.1002/pro.3715> (2019).
25. Kanehisa, M. *et al.* KEGG for taxonomy-based analysis of pathways and genomes. *Nucleic Acids Res.* **51**(D1), D587–D592. <https://doi.org/10.1093/nar/gkac963> (2023).
26. Cheng, J. *Study on Active Ingredients of Five-Finger Hairy Peach* (Guangdong Pharmaceutical University, 2017).
27. Huang, P. *et al.* *J. Liaoning Univ. Tradit. Chin. Med.*, **22**(12):93–96 (2020). <https://doi.org/10.13194/j.issn.1673-842x.2020.12.022>
28. Lao, J. L. *et al.* Research progress on chemical composition and pharmacological effects of *P. pentaciensis*. *J. Trop. Agric. Sci.* **38**(05), 82–87 (2018).
29. Zhao, S. *et al.* Research progress on chemical composition, pharmacological effects and prediction analysis of quality markers of Yaoyao five-finger hairy peach. *World Sci. Technol. Mod. Tradit. Chin. Med.* **22**(05), 1506–1516 (2020).
30. Ye, T. *et al.* Research progress on chemical composition and pharmacological activity of five-finger hairy peach. *J. Guangdong Pharm. Univ.* **35**(04), 591–596. <https://doi.org/10.16809/j.cnki.2096-3653.2019030401> (2019).
31. Lv, Z., Chen, K. & Peng, Y. H. Chinese Journal of Tropical Crops, **38**(6):4. <https://doi.org/10.3969/j.issn.1000-2561.2017.06.024> (2017)
32. Chen, C., Chen, J. & Wan, C. Pinocembrin-7-glucoside (P7G) reduced postharvest blue mold of navel orange by suppressing *Penicillium italicum* growth. *Microorganisms* **8**(4), 536. <https://doi.org/10.3390/microorganisms8040536> (2020).
33. Zhang, R., Qu, Z. Y. & Du, J. Exploring the antioxidant protection mechanism of *P. chinensis* extract on mice with alcoholic liver injury based on Nrf2-HO-1/CYP2E1 pathway. *New Drugs Clin. Pharmacol. Tradit. Chin. Med.* **32**(12), 1769–1775. <https://doi.org/10.19378/j.issn.1003-9783.2021.12.006> (2021).
34. Zhou, T. N. *et al.* Study on anti-inflammatory, analgesic and protective effects of *P. pentachi* on acute liver injury. *Pharm. Sci. Today.* (02): 55–58 (2008).
35. Huang, P. W. *et al.* Research progress on chemical composition, pharmacological effects and clinical application of Chinese medicine five-finger hairy peach. *J. Liaoning Univ. Tradit. Chin. Med.* **22**(12), 93–96. <https://doi.org/10.13194/j.issn.1673-842x.2020.12.022> (2020).
36. Gui, Q. *et al.* Study on active components in different leaf types of *P. chinensis* under rubber plantation. *Food Ind.* **39**(11), 188–191 (2018).
37. Lv, Z. C., Chen, K. & Peng, Y. H. Isolation and identification of anti-inflammatory active components of five-fingered hairy peach. *Chin. J. Trop. Crops* **38**(06), 1134–1137 (2017).
38. Cai, Q. Y. *et al.* Study on the hepatotoxic effect and active components of cocaine antagonistic drug cocaine. *Chin. J. Tradit. Chin. Med.* **12**, 1190–1193 (2007).
39. Ye, T. *et al.* Research progress on chemical composition and pharmacological activity of five-fingered hairy peach. *J. Guangdong Pharm. Univ.* **35**(04), 591–596. <https://doi.org/10.16809/j.cnki.2096-3653.2019030401> (2019).

40. Tan, M. *et al.* Antitumor effect of psoralen on MCF-7 cells of breast cancer in vitro. *Guangdong Med. J.* **11**, 1817–1819. <https://doi.org/10.13820/j.cnki.gdyx.2008.11.079> (2008).
41. Pan, Y. M., Wang, J. H., Fang, J. & Wang, R. Pathological morphological effect of psoralen on hippocampal region of brain tissue in rats with ovarian dementia. *China Contemp. Med.* **23**(26), 9–11 (2016).
42. Zhang, Y. H. *et al.* Immunomodulatory effect of psoralen on mouse model of rheumatoid arthritis. *Chin. J. Lab. Zool.* **25**(02), 207–210 (2017).
43. Geng, D. D., Zhao, B. & Wang, J. H. Effects of bergamot lactone on proliferation and differentiation of rat osteoblasts. *Nat. Prod. Res.* **29**(09), 1563–1567. <https://doi.org/10.16333/j.1001-6880.2017.9.019> (2017).
44. Yang, K., Gao, Q. & Maia, Z. Research progress on pharmacological effects and hepatotoxicity mechanism of psoralens. *Chin. Trad. Herb. Drugs.* **52**(01), 289–298 (2021).
45. Xie, S. H. & Feng, M. R. Research progress on pharmacological effects of bergamot lactone. *J. Hainan Med. Coll.* **28**(24), 1917–1920. <https://doi.org/10.13210/j.cnki.jhmu.20210507.003> (2022).
46. Wang, Y. *et al.* Research progress on MYB transcription factors regulating phenylpropanoid biosynthesis. *J. Anhui Agric. Univ.* **46**(05), 859–864. <https://doi.org/10.13610/j.cnki.1672-352x.20191122.018> (2019).
47. Falcone Ferreyra, M. L., Rius, S. P. & Casati, P. Flavonoids: Biosynthesis, biological functions, and biotechnological applications. *Front. Plant Sci.* **3**(222), 222. <https://doi.org/10.3389/fpls.2012.00222> (2012).

Acknowledgements

We are grateful to the Lingnan Medical Research Center of Guangzhou University of Traditional Chinese Medicine and The First Affiliated Hospital of Guangzhou University of Traditional Chinese Medicine for providing technical support for the study of traditional Chinese medicine.

Author contributions

Conceptualization, K.X.G. and X.H.K.; methodology, K.X.G. and X.H.K.; software, K.X.G. validation, K.X.G., Y.F.L. and X.H.K.; formal analysis, K.X.G.; investigation, X.C.Y., H.T., H.Y.W. and Y.L.; resources, X.H.K. and X.C.Y.; data curation, K.X.G.; writing—original draft preparation, K.X.G.; writing—review and editing, K.X.G. and X.H.K.; visualization, W.Z. and X.H.K.; supervision, W.Z. and X.H.K.; project administration, and X.H.K. and X.C.Y.; funding acquisition, X.H.K. and X.C.Y. All authors have read and agreed to the published version of the manuscript. Author contributions.

Funding

This research was funded by the National Natural Science Foundation of China, China, Grant Number: 82074099; Guangdong Natural Science Foundation Project, China, Grant Number: 2023A1515011126; Guangdong Provincial Bureau of Traditional Chinese Medicine Research Project, China, Grant Number: 20201404; and, Qingyuan City Science and Technology Plan Project, China, Grant Number: 2021SJXM025.

Competing interests

The authors declare no competing interests.

Additional information

Correspondence and requests for materials should be addressed to Y.L. or X.-H.K.

Reprints and permissions information is available at www.nature.com/reprints.

Publisher's note Springer Nature remains neutral with regard to jurisdictional claims in published maps and institutional affiliations.



Open Access This article is licensed under a Creative Commons Attribution 4.0 International License, which permits use, sharing, adaptation, distribution and reproduction in any medium or format, as long as you give appropriate credit to the original author(s) and the source, provide a link to the Creative Commons licence, and indicate if changes were made. The images or other third party material in this article are included in the article's Creative Commons licence, unless indicated otherwise in a credit line to the material. If material is not included in the article's Creative Commons licence and your intended use is not permitted by statutory regulation or exceeds the permitted use, you will need to obtain permission directly from the copyright holder. To view a copy of this licence, visit <http://creativecommons.org/licenses/by/4.0/>.

© The Author(s) 2024